Available online at www.sciencedirect.com

ScienceDirect

IFAC Papers Online CONFERENCE PAPER ARCHIVE

IFAC PapersOnLine 55-36 (2022) 306–311

Multi-vehicle Conflict Management under Time Delays

Hao M. Wang *, **Sergei S. Avedisov** **, **Onur Altintas** **, **Gábor Orosz** *,***

* *Department of Mechanical Engineering, University of Michigan, Ann Arbor, MI 48109, USA. ({haowangm, orosz}@umich.edu).*
** *Toyota Motor North America R&D InfoTech Labs, Mountain View, CA 94043, USA. ({sergei.avedisov, onur.altintas}@toyota.com).*
*** *Department of Civil and Environmental Engineering, University of Michigan, Ann Arbor, MI 48109, USA.*

Abstract: This paper extends the framework for conflict resolution to multiple vehicles with different automation levels, while considering time delays in vehicle dynamics and in vehicle-to-everything (V2X) communication. Using reachability analysis, we interpret the V2X-based vehicle status information to enable real-time decision making and control of a connected automated vehicle interacting with multiple connected vehicles. We reveal the effects of time delays in such mixed-autonomy environment, and demonstrate the effectiveness of the proposed conflict resolution strategies using simulations with real highway traffic data.

Keywords: Connected and automated vehicles, Conflict resolution, Time delay, V2X communication, Goal-oriented control.

1. INTRODUCTION

Cooperative maneuvering of road users may involve conflicts when their trajectories intersect or they come sufficiently close. Detection and resolution of such conflicts in a timely manner to ensure traffic safety and efficiency has attracted considerable research attention. Prior studies show that in a fully automated environment, vehicle-to-everything (V2X) communication may enable vehicles to negotiate and agree on their future maneuvers, and thus, manage conflicts in a cooperative manner; see Liu et al. (2020); Hafner et al. (2013); Rios-Torres and Malikopoulos (2016).

In the next few decades, however, we expect a mixed-autonomy environment where vehicles of different automation levels and cooperation classes coexist; see SAE J3016 (2021); SAE J3216 (2021). Methods such as model predictive control (Karimi et al., 2020), reachability analysis (Bajcsy et al., 2019), and game theory (Albaba and Yildiz, 2019) were used for decision making and control design in such mixed traffic scenarios. Our previous results reported in Wang et al. (2020, 2021, 2022a,b) established a tool called conflict analysis to resolve conflicts in mixed-autonomy environments, where vehicles share their current status (e.g., GPS position and velocity), and their intent about future trajectories (e.g., velocity and/or acceleration bounds of their future motion) via V2X. Conflict analysis allows one to detect and resolve conflicts preemptively and analyze the merits of different cooperation classes for conflict resolution. In this paper, we focus on investigating the effects that time delays in vehicle dynamics and in V2X communication have on conflicts.

Figure 1(a)-(b) show a maneuver involving potential conflicts where an ego vehicle attempts to move into the right lane between two remote vehicles on a highway. Such lane change maneuvers consist of two steps: (i) the ego vehicle forms appropriate front and rear distances from the remote vehicles while staying in its current lane; (ii) the ego vehicle moves into the target lane by changing its lateral position. Here we focus on step (i) and assume that step (ii) is carried out by lateral motion planners afterwards. We define two rectangle-shaped conflict zones to represent the safety buffers between the ego vehicle and two remote vehicles; see the red shaded areas in Fig. 1. These conflict zones move together with the corresponding remote vehicles and their sizes may vary according to road configurations. To prevent conflict, the ego vehicle must form necessary front and rear gaps such that it does not overlap with the two conflict zones.

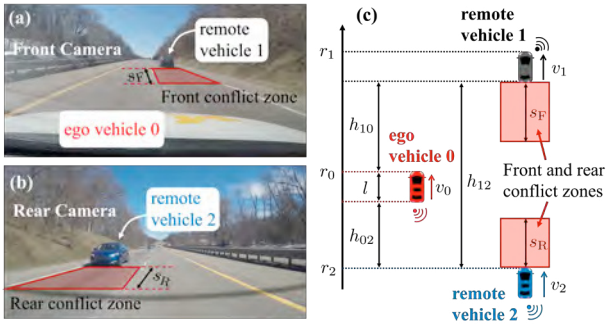

Fig. 1. Lane change maneuver involving three vehicles with potential conflicts. (a-b) Front and rear camera views from the ego vehicle 0 at the moment when it decides to move into the target lane between remote vehicle 1 and remote vehicle 2; (c) Generalized model where the red-shaded regions highlight the front and rear conflict zones.

10.1016/j.ifacol.2022.11.375

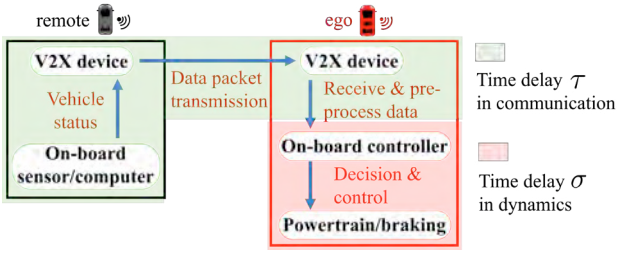

Fig. 2. Time delays in the ego vehicle's dynamics and in the V2X communication between ego and remote vehicles.

We resolve conflicts from the perspective of the ego vehicle, assuming that all vehicles are equipped with vehicle-to-vehicle (V2V) communication devices that transmit and receive messages containing their most recently measured position and velocity. We refer to such V2V communication as status-sharing communication. An example of standardized status-sharing communication is the Basic Safety Messages (BSMs); see SAE J2735 (2016). As shown in Fig. 2, we consider two types of time delays in the system. Communication delay (highlighted by green shading) is associated with compiling the V2X message on the remote vehicle, transmitting this message, and pre-processing the received data on the ego vehicle. Time delay in the dynamics of the ego vehicle (indicated by red shading) results from on-board computation time, and from the actuation time in the powertrain and braking systems.

While incorporating these time delays, we propose a reachability-based method to investigate whether a conflict is preventable based on available vehicle status information. This allows for efficient and reliable decision making, motion planning and control. We propose a so-called goal-oriented controller for the ego vehicle to pursue an appropriately selected goal state while guaranteeing a conflict-free maneuver. The effects of time delays on conflict resolution are quantified, and the effectiveness of the extended conflict analysis framework is demonstrated using real highway data.

2. MODELING VEHICLE DYNAMICS AND COMMUNICATION

Consider the scenario in Fig. 1(a-b) where the ego vehicle 0 attempts to move into the target lane in between remote vehicles 1 and 2. As mentioned before, we focus on the first step of the lane change maneuver, where the ego vehicle forms the necessary longitudinal gaps before crossing the lane markings laterally. The conflict zone lengths s_{F} and s_{R} represent minimal front and rear distances the ego vehicle must secure to ensure a conflict-free lane change. Considering the restricted velocity ranges in typical highway driving scenarios, we adopt a reasonable simplification of constant s_{F} and s_{R}; see Table 1. This is used to better highlight the main idea of conflict analysis, while the results can be easily adapted to non-constant s_{F} and s_{R}. Fig. 1(c) shows the generalized model where r_0, r_1 and r_2 denote the positions of the vehicles' front bumpers, and v_0, v_1 and v_2 denote their longitudinal velocities.

By neglecting the air and rolling resistances, the longitudinal dynamics of the vehicles can be described by

$$\begin{aligned} \dot{r}_0(t) &= v_0(t), \quad \dot{v}_0(t) = \mathrm{sat}(u_0(t-\sigma)), \\ \dot{r}_i(t) &= v_i(t), \quad \dot{v}_i(t) = \mathrm{sat}(u_i(t)), \quad i = 1, 2. \end{aligned} \tag{1}$$

where the dot denotes the derivative with respect to time t, and the control inputs u_0, u_1 and u_2 are subject to the saturation function

$$\mathrm{sat}(u) = \max\big\{\min\{u, a_{\max}\}, a_{\min}\big\}, \tag{2}$$

which contain the acceleration limits $a_{\min}$ and $a_{\max}$. For $v = v_{\min}$, we substitute $a_{\min}$ with 0, since the vehicle shall not decelerate; for $v = v_{\max}$, we substitute $a_{\max}$ with 0, since the vehicle shall not accelerate. Here we use limits corresponding to typical highway driving behaviors, and assume that these values are known to the ego vehicle; see Table 1. We use σ to denote the time delay in the ego vehicle's dynamics, which comes from its on-board controller and the powertrain/braking system; see the red-shaded part in Fig. 2. The delays in the dynamics of the remote vehicles are not explicitly considered, to represent the ego vehicle's limited knowledge about the remote vehicles' dynamics. However, as will be shown further below, our analysis implicitly handles such delays. Note that we do not have control over the remote vehicles' motions, i.e., cannot prescribe inputs u_1 and u_2.

We consider that the vehicles share their status information via V2X communication, i.e., the positions r_1, r_2 and velocities v_1, v_2 of the remote vehicles are made available to the ego vehicle, and are used in decision making and in determining the control input u_0. However, as highlighted by the green-shaded part in Fig. 2, time delays exist in the communication between the remote and ego vehicles due to on-board computation, data transmission and processing. We use τ_1 and τ_2 to denote the communication delays of remote vehicles 1 and 2, and assume that the values of τ_1 and τ_2 are known to the ego vehicle. This is a reasonable assumption since the messages are time stamped. When the ego vehicle receives status messages from the remote vehicles at a given time t, only delayed status $r_1(t-\tau_1)$, $r_2(t-\tau_2)$, $v_1(t-\tau_1)$, and $v_2(t-\tau_2)$ are available. Without loss of generality, we assume the status of both remote vehicles are received in a synchronized manner and define the initial time $t = 0$ as the time when the first pair of status packets are received by the ego vehicle.

We define the relative distances between vehicles as

$$h_{10} := r_1 - r_0 - l, \quad h_{02} := r_0 - r_2 - l, \quad h_{12} := r_1 - r_2 - l, \tag{3}$$

where h_{10} and h_{02} are the front and rear gaps between the ego vehicle 0 and remote vehicles 1 and 2, respectively, and h_{12} is the total gap between the two remote vehicles; see Fig. 1(c). We assume that all vehicles have length l. Note that $h_{12} = h_{10} + h_{02} + l \geq 0$ because the remote vehicle 2 is assumed to travel behind vehicle 1. This leads to $h_{10} + h_{02} \geq -l$. Since relative distances (3) play a key role in lane change maneuvers, we define the state of the system (1) as

$$\mathbf{x} := [h_{10}, h_{02}, v_0, v_1, v_2]^\top \in \Omega, \tag{4}$$

where the domain Ω is given by

$$\begin{aligned} \Omega := &\{[h_{10}, h_{02}]^\top \in \mathbb{R}^2 | h_{10} + h_{02} \geq -l\} \times [v_{\min,0}, v_{\max,0}] \\ &\times [v_{\min,1}, v_{\max,1}] \times [v_{\min,2}, v_{\max,2}]. \end{aligned} \tag{5}$$

Table 1. Parameters values used in the paper.

s_{F}, s_{R}	10 [m]	l	5 [m]
$a_{\min,0}$	-8 [m/s^2]	$a_{\min,1}$, $a_{\min,2}$	-4 [m/s^2]
$a_{\max,0}$	4 [m/s^2]	$a_{\max,1}$, $a_{\max,2}$	2 [m/s^2]
$v_{\min,0}$	22 [m/s]	$v_{\min,1}$, $v_{\min,2}$	25 [m/s]
$v_{\max,0}$	38 [m/s]	$v_{\max,1}$, $v_{\max,2}$	35 [m/s]

3. CONFLICT ANALYSIS

In this section we establish conflict analysis in the presence of time delays. We use formal logic to provide a rigorous description of conflict, and then propose a reachability analysis-based method to determine whether a conflict is preventable based on vehicle status information. We also quantify the effects of delays arising in the dynamics and due to V2X communication.

Before changing lanes, the ego vehicle must secure the necessary front and rear gaps. Such a conflict-free maneuver can be formally described by the proposition

$$P := \{\exists t \geq 0, h_{10}(t) \geq s_{\mathrm{F}} \wedge h_{02}(t) \geq s_{\mathrm{R}}\}, \tag{6}$$

where the symbol $\wedge$ (and) is used. Proposition P can be further decomposed into three cases:

(i) No-conflict: ego vehicle 0 is able to prevent conflict independent of the motion of remote vehicles 1 & 2.
(ii) Uncertain: ego vehicle 0 may be able to prevent conflict depending on the motion of remote vehicles 1 & 2.
(iii) Conflict: ego vehicle 0 is unable to prevent conflict independent of the motion of remote vehicles 1 & 2.

These cases correspond to three pairwise disjoint sets in the state space Ω of system (1):

$$\mathcal{P}_{\mathrm{g}} := \{\mathbf{x}(0) \in \Omega | \forall u_1(t), \forall u_2(t), \exists u_0(t), P\}, \tag{7}$$

$$\mathcal{P}_{\mathrm{y}} := \{\mathbf{x}(0) \in \Omega | (\exists u_1(t), \exists u_2(t), \forall u_0(t), \neg P) \wedge (\exists u_1(t), \exists u_2(t), \exists u_0(t), P)\}, \tag{8}$$

$$\mathcal{P}_{\mathrm{r}} := \{\mathbf{x}(0) \in \Omega | \forall u_1(t), \forall u_2(t), \forall u_0(t), \neg P\}, \tag{9}$$

where the symbol $\neg$ means negation, and $u_0(t)$, $u_1(t)$, and $u_2(t)$ are functions of time $t \geq 0$. Noting that the first and second predicates in (8) are the negations of the predicates in (7) and (9), we have $\mathcal{P}_{\mathrm{g}} \cup \mathcal{P}_{\mathrm{y}} \cup \mathcal{P}_{\mathrm{r}} = \Omega$. We remark that $\mathcal{P}_{\mathrm{r}} = \emptyset$ holds under a reasonable condition of behavior parameters $(v_{\max,1} > v_{\min,2}) \wedge (v_{\max,0} > v_{\min,2}) \wedge (v_{\min,0} < v_{\max,1})$; see Table 1. This condition allows the remote vehicles to make large enough total gap (if vehicle 1 accelerates and vehicle 2 slows down) so that the ego vehicle is able to move in eventually without conflict. Thus, in the rest of this section, we focus on $\mathcal{P}_{\mathrm{g}}$ and $\mathcal{P}_{\mathrm{y}}$.

3.1 Conflict analysis with time delay in dynamics

In this subsection, we consider time delay in the ego vehicle's dynamics while ignoring the communication delays for both remote vehicles. We provide a method to check whether an initial state $\mathbf{x}(0)$ belongs to set $\mathcal{P}_{\mathrm{g}}$ or $\mathcal{P}_{\mathrm{y}}$.

If $h_{10}(0) \geq s_{\mathrm{F}} \wedge h_{02}(0) \geq s_{\mathrm{R}}$, we have $\mathbf{x}(0) \in \mathcal{P}_{\mathrm{g}}$ immediately since the ego vehicle already formed necessary front and rear gaps at the initial time; otherwise, one needs to check if proposition P is true for some $t > 0$, considering all possible future behaviors of the ego and remote vehicles. The Lemma below demonstrates that the behavior limits of the remote vehicles need to be used when checking $\mathbf{x}(0) \in \mathcal{P}_{\mathrm{g}}$; see Wang et al. (2022a) for the proof.

Lemma 1. The following relationship holds for any given initial state $\mathbf{x}(0) \in \Omega$:

$$\{\forall u_1(t), \forall u_2(t), \exists u_0(t), P\} \iff \{(u_1(t), u_2(t)) \equiv (a_{\min,1}, a_{\max,2}), \exists u_0(t), \exists t \in T, h_{10}(t) \geq s_{\mathrm{F}} \wedge h_{02}(t) \geq s_{\mathrm{R}}\}, \tag{10}$$

where $T = \{t \geq 0 | h_{12}(t) \geq s_{\mathrm{F}} + s_{\mathrm{R}} + l\}$.

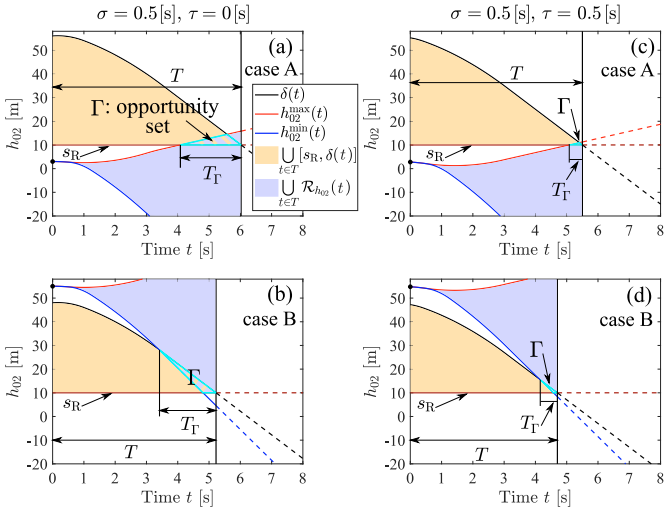

Fig. 3. (a)-(b) Opportunity set Γ for initial velocities $(v_0(0), v_1(0), v_2(0)) = (28, 29, 28)$[m/s] and initial front and rear gaps $(h_{10}(0), h_{02}(0)) = (63, 3)$[m] for case A and $(h_{10}(0), h_{02}(0)) = (3, 55)$[m]. The control input history of ego vehicle is $u_0(t) = 0\,[\mathrm{m/s^2}], t \in [-\sigma, 0]$. (c)-(d) Opportunity set Γ under additional communication delays using estimated initial velocities $(v_0(0), v_1^{\mathrm{est}}(0), v_2^{\mathrm{est}}(0)) = (28, 26.7, 28.85)$[m/s] and estimated initial front and rear gaps $(h_{10}^{\mathrm{est}}(0), h_{02}^{\mathrm{est}}(0)) = (62.43, 2.79)$[m] for case A and $(h_{10}^{\mathrm{est}}(0), h_{02}^{\mathrm{est}}(0)) = (2.43, 54.79)$[m] for case B.

Here T represents a time interval within which the ego vehicle must form the necessary front and rear gaps to prevent conflicts, under the worst-case behaviors of the remote vehicles (given by their input limits). Thus, checking $\mathbf{x}(0) \in \mathcal{P}_{\mathrm{g}}$ is equivalent to examining the existence of an input $u_0(t)$ and a time $t \in T$ such that $h_{10}(t) \geq s_{\mathrm{F}} \wedge h_{02}(t) \geq s_{\mathrm{R}}$ holds assuming the remote vehicles' worst-case behaviors. Due to the delay σ in the dynamics, the control input assigned to the ego vehicle only acts after σ time. Thus, the ego vehicle's motion during the time interval $t \in [0, \sigma]$ is determined by its control input history $u_0(t), t \in [-\sigma, 0]$. Also notice that the worst-case behavior assumption about the remote vehicles' motion implicitly considers the effects of the unknown delays in their dynamics. The following Theorem provides a reachability-based criterion to check $\mathbf{x}(0) \in \mathcal{P}_{\mathrm{g}}$.

Theorem 1. Given the dynamics (1,2) and the initial state $\mathbf{x}(0) \in \Omega$, $\mathbf{x}(0) \in \mathcal{P}_{\mathrm{g}}$ holds if and only if the condition

$$\Gamma := \bigcup_{t\in T}[s_{\mathrm{R}}, \delta(t)] \cap \bigcup_{t\in T}\mathcal{R}_{h_{02}}(t) \neq \emptyset, \tag{11}$$

is satisfied under $(u_1(t), u_2(t)) \equiv (a_{\min,1}, a_{\max,2})$, where $\delta(t) = h_{12}(t) - s_{\mathrm{F}} - l$, $\mathcal{R}_{h_{02}}(t) = [h_{02}^{\min}(t), h_{02}^{\max}(t)]$.

The analytical form of $\delta(t)$, $h_{02}^{\min}(t)$, and $h_{02}^{\max}(t)$ are given in Appendix A while the proof is given in Appendix B. The set $\bigcup_{t\in T}[s_{\mathrm{R}}, \delta(t)]$ contains the time t and the rear gap h_{02} such that $h_{10}(t) \geq s_{\mathrm{F}} \wedge h_{02}(t) \geq s_{\mathrm{R}}$ under the worst-case behaviors of remote vehicles, while ignoring the ego vehicle's capability. On the other hand, the set $\bigcup_{t\in T}\mathcal{R}_{h_{02}}(t)$ gives all rear gap values that the ego vehicle is able to reach while taking into account the delay σ, i.e., the projection of the reachable tube of system (1) to (t, h_{02}); see Haddad

and Halder (2020) for examples of reachable sets and tubes. Thus, the set Γ collects all feasible rear gaps and the corresponding times when the ego vehicle can secure $h_{10}(t) \geq s_{\mathrm{F}} \wedge h_{02}(t) \geq s_{\mathrm{R}}$. We call Γ the opportunity set and denote the time window it covers by T_Γ. These sets are depicted in Fig. 3(a) where the black curve is computed using $(u_1(t), u_2(t)) \equiv (a_{\min,1}, a_{\max,2})$, while the red and blue curves are computed using $(u_0(t), u_2(t)) \equiv (a_{\max,0}, a_{\max,2})$ and $(u_0(t), u_2(t)) \equiv (a_{\min,0}, a_{\max,2})$ for $t > 0$, respectively, with the given control input history $u_0(t)$, $t \in [-\sigma, 0]$.

We emphasize that Theorem 1 converts the checking of $\mathbf{x}(0) \in \mathcal{P}_{\mathrm{g}}$ to the checking of intersection of two analytically given sets. This can be done efficiently with numerical methods and is suitable for real-time implementation. For more complex dynamics, the set $\mathcal{R}_{h_{02}}(t)$ may not be expressed analytically, and one may utilize approximation techniques to compute reachable sets; see Kochdumper and Althoff (2021). Fig. 3(a)-(b) show two cases when $\Gamma \neq \emptyset$ under delay $\sigma = 0.5$ [s] as indicated by the striped regions. These correspond to initial states $\mathbf{x}(0) \in \mathcal{P}_{\mathrm{g}}$ when the ego vehicle is initially behind and in front of the remote vehicles, respectively. If $\mathbf{x}(0) \in \mathcal{P}_{\mathrm{g}}$, conflict can be avoided, so the ego vehicle's decision is to change lane. If $\mathbf{x}(0) \in \mathcal{P}_{\mathrm{y}}$, it may not be able to change lanes without conflict, and thus, the decision is to keep its current lane.

By denoting the opportunity set and the time window it covers under a larger delay $\hat{\sigma} \geq \sigma$ as $\hat{\Gamma}$ and $\hat{T}_\Gamma$, we have

$$\Gamma \supseteq \hat{\Gamma}, \quad T_\Gamma \supseteq \hat{T}_\Gamma. \tag{12}$$

That is, the opportunity set shrinks as the delay increases, leading to smaller opportunity window for conflict-free maneuver. This will be quantified further below in Fig. 4.

3.2 Conflict analysis with time delays in communication

In this subsection, we extend conflict analysis by considering communication delays in the status information received from remote vehicles.

Under communication delays τ_1 and τ_2 associated with remote vehicles 1 and 2, at the initial time, the ego vehicle has access to its own current status $r_0(0)$, $v_0(0)$, and the remote vehicles' delayed status $r_1(-\tau_1)$, $v_1(-\tau_1)$, $r_2(-\tau_2)$, and $v_2(-\tau_2)$. That is, the exact initial state $\mathbf{x}(0)$ is not available to the ego vehicle, and thus, checking $\mathbf{x}(0) \in \mathcal{P}_{\mathrm{g}}$ is not implementable. Note that while the communication delays compromise the ego vehicle's awareness of the exact current state, the sets $\mathcal{P}_{\mathrm{g}}$ and $\mathcal{P}_{\mathrm{y}}$ are still based on the current state which needs to be estimated. Since the ego vehicle has no knowledge about the actual behaviors of the remote vehicles during the time intervals $t \in [-\tau_1, 0]$ and $t \in [-\tau_2, 0]$, we modify the propositions for no conflict and uncertain cases in (7) and (8) as

$$\tilde{P}_{\mathrm{g}} := \tag{13}$$
$$\{\forall u_1(t) \,\mathrm{on}\, t \geq -\tau_1, \forall u_2(t) \,\mathrm{on}\, t \geq -\tau_2, \exists u_0(t) \,\mathrm{on}\, t \geq 0, P\},$$

$$\tilde{P}_{\mathrm{y}} := \tag{14}$$
$$\{\exists u_1(t) \,\mathrm{on}\, t \geq -\tau_1, \exists u_2(t) \,\mathrm{on}\, t \geq -\tau_2, \forall u_0(t) \,\mathrm{on}\, t \geq 0, \neg P\} \wedge$$
$$\{\exists u_1(t) \,\mathrm{on}\, t \geq -\tau_1, \exists u_2(t) \,\mathrm{on}\, t \geq -\tau_2, \exists u_0(t) \,\mathrm{on}\, t \geq 0, P\}.$$

In fact, one can prove the following relationships

$$\tilde{P}_{\mathrm{g}} \iff \mathbf{x}_{\mathrm{est}}(0) \in \mathcal{P}_{\mathrm{g}}, \tag{15}$$
$$\tilde{P}_{\mathrm{y}} \iff \mathbf{x}_{\mathrm{est}}(0) \in \mathcal{P}_{\mathrm{y}}, \tag{16}$$

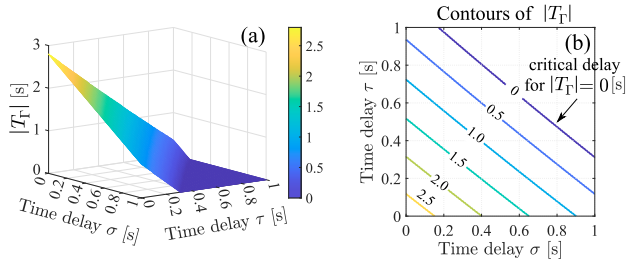

Fig. 4. Time window as function of the delay σ arising in the dynamics and the communication delay τ for case B in Fig. 3. (a) 3D surface; (b) contours plot.

where $\mathbf{x}_{\mathrm{est}}(0)$ is the estimated initial state based on the $r_0(0)$, $v_0(0)$, $r_1(-\tau_1)$, $v_1(-\tau_1)$, $r_2(-\tau_2)$, and $v_2(-\tau_2)$, using $u_1(t) \equiv a_{\min,1}$, $t \in [-\tau_1, 0]$ and $u_2(t) \equiv a_{\max,2}$, $t \in [-\tau_2, 0]$. That is, by estimating the current state, the methodology introduced in the previous subsection can be applied to determine whether a conflict is preventable under communication delays.

Figure 3(c)-(d) show the opportunity set when adding the communication delays $\tau_1 = \tau_2 = \tau = 0.5$ [s] with the estimated initial states $\mathbf{x}_{\mathrm{est}}(0)$ based on (15)-(16) such that the true initial states $\mathbf{x}(0)$ still correspond to cases A and B in Fig. 3(a)-(b). The remote vehicles' actual behaviors are given by $(u_1(t), u_2(t)) = (0.6, 0.3)[\mathrm{m/s^2}], t \in [-\tau, 0]$. The opportunity sets shrink under additional communication delay due to the conservatism in $\mathbf{x}_{\mathrm{est}}(0)$. By denoting the opportunity set and the time window it covers under a larger communication delay $\tilde{\tau} \geq \tau$ by $\tilde{\Gamma}$ and $\tilde{T}_\Gamma$, we have

$$T_\Gamma \supseteq \tilde{T}_\Gamma, \quad |\Gamma(t)| \geq |\tilde{\Gamma}(t)|, \quad \forall t \in T_\Gamma, \tag{17}$$

where $\Gamma(t)$ and $\tilde{\Gamma}(t)$ are slices of Γ and $\tilde{\Gamma}$ at time t, and $|\cdot|$ measures the length of one-dimensional set. Note that although $\Gamma \supseteq \tilde{\Gamma}$ does not hold in general, (17) implies that as communication delay increases, the ego vehicle expects less opportunity for conflict-free maneuver.

The 3D surface in Fig. 4(a) illustrates the time window length $|T_\Gamma|$ as a function of the delay σ in the dynamics and communication delay τ for the initial state case B in Fig. 3. Fig. 4(b) shows the contours of $|T_\Gamma|$ in the (σ, τ)-plane. The contour $|T_\Gamma| = 0$ gives the critical combinations of delays σ and τ such that the opportunity set disappears, i.e., a conflict-free lane change can no longer be guaranteed for larger delay values. Note that the gradient of the 3D surface and the critical delay combination depend on the initial states, but the qualitative behaviors remain similar.

4. CONTROLLER DESIGN AND SIMULATION

In this section, we propose a controller for the ego vehicle to form necessary longitudinal gaps for conflict-free lane changes under both dynamics and communication delays. Then we demonstrate the effectiveness of the conflict analysis framework using simulations with real traffic data.

For $\mathbf{x}(0) \in \mathcal{P}_{\mathrm{g}}$ (or $\mathbf{x}_{\mathrm{est}}(0) \in \mathcal{P}_{\mathrm{g}}$ with communication delay), the opportunity set $\Gamma \neq \emptyset$ and each point $(t, h_{02}) \in \Gamma$ gives a feasible rear gap and a corresponding time assuming the worst-case behaviors of the remote vehicles. Once this rear gap is formed, the necessary front gap is also guaranteed simultaneously. Thus, the control input $u_0(t)$ can be designed by selecting an appropriate goal point $(t^{\mathrm{G}}, h_{02}^{\mathrm{G}}) \in \Gamma$.

We call this goal-oriented control. From the perspective of robustness, we select the "center point" of the opportunity set as the goal, i.e., choose t^{G} in the middle of T_Γ and h_{02}^{G} in the middle of the slice $\Gamma(t^{\mathrm{G}})$; see the black point in Fig. 5(a). We design a constant value control input $u_0(t) = u_0^{\mathrm{G}}$ for the ego vehicle to pursue the goal point $(t^{\mathrm{G}}, h_{02}^{\mathrm{G}})$ while assuming the worst-case behaviors of the remote vehicles whose analytical form is given in Appendix C. The gray arrow in Fig. 5(a) depicts the expected trajectory $h_{02}(t)$ under the designed constant-value input. We emphasize that the domain $\mathcal{P}_{\mathrm{g}}$ is invariant under the goal-oriented controller u_0^{G} independent of remote vehicles' motions in the presence of delays. Once status updates are received from the remote vehicles, the opportunity set Γ is recalculated, and the goal point $(t^{\mathrm{G}}, h_{02}^{\mathrm{G}}) \in \Gamma$ and the corresponding control input u_0^{G} are also updated.

For the remote vehicles we utilize data collected from real human-driven vehicles involved in a lane change maneuver on highway I-94 in southeast Michigan; see Fig. 1(a)-(b). During this maneuver, remote vehicle 2 travels faster than remote vehicle 1, and the total gap between remote vehicles shortens; see the acceleration, speed, and distance data in Fig. 5(e)-(g). The ego vehicle is a connected automated vehicle attempting to move into the target lane between the two connected remote vehicles. We consider dynamics delay $\sigma = 0.5\,[\mathrm{s}]$ for the ego vehicle with control input history $u_0(t) = 1\,[\mathrm{m/s^2}], t \in [-\sigma, 0]$ and communication delays $\tau_1 = \tau_2 = \tau = 0.1\,[\mathrm{s}]$. At the initial time, the ego vehicle has access to vehicle status $(r_0(0), r_1(-0.1), r_2(-0.1)) = (0, 68.94, -7.61)\,[\mathrm{m}]$ and $(v_0(0), v_1(-0.1), v_2(-0.1)) = (35.58, 32.46, 32.82)\,[\mathrm{m/s}]$. The estimated initial front and rear gaps are $h_{10}^{\mathrm{est}}(0) = 67.16\,[\mathrm{m}]$ and $h_{02}^{\mathrm{est}}(0) = -0.68\,[\mathrm{m}]$, while the estimated initial speeds of remote vehicles become $v_1^{\mathrm{est}}(0) = 32.06\,[\mathrm{m/s}]$ and $v_2^{\mathrm{est}}(0) = 33.02\,[\mathrm{m/s}]$. This yields $\mathbf{x}_{\mathrm{est}}(0) \in P_{\mathrm{g}}$ and the ego vehicle decides to pursue the lane change opportunity by using the goal-oriented controller $u_0(t) = u_0^{\mathrm{G}}$. Note that the value of u_0^{G} is updated each time a status update is received.

Fig. 5(a)-(d) illustrate the evolution of opportunity set Γ, the goal point $(t^{\mathrm{G}}, h_{02}^{\mathrm{G}}) \in \Gamma$, and trajectory $h_{02}(t)$ (magenta curve), when status of remote vehicles are updated every 0.1 [s]. The corresponding time profiles are shown in Fig. 5(e)-(g). The opportunity set expands under status updates since the actual behaviors of remote vehicles do not follow the worst-case scenario. Thus, frequent status updates improve the ego vehicle's prediction in real time and mitigate the conservatism in conflict analysis. At 3.6[s], the ego vehicle forms the necessary gaps, and the lateral lane change can be initiated. That is, the goal point serves as a guidance for the ego vehicle's motion until sufficient relative distances are formed.

5. CONCLUSION

In this paper we studied conflict resolution involving connected vehicles with different automation levels. The presence of delays in vehicle-to-vehicle communication and vehicle dynamics required the extension of the conflict analysis framework to account for these delays. We designed a goal-oriented controller which guarantees conflict-free maneuvers in the presence of time delays. We demonstrated the effectiveness of the proposed conflict analysis framework and the control strategy by simulations using real highway data. Our future work include investigating different classes of vehicle cooperation. Furthermore, we plan to extend the framework to more general vehicle dynamics models, and to validate the goal-oriented controller through real-vehicle experiments.

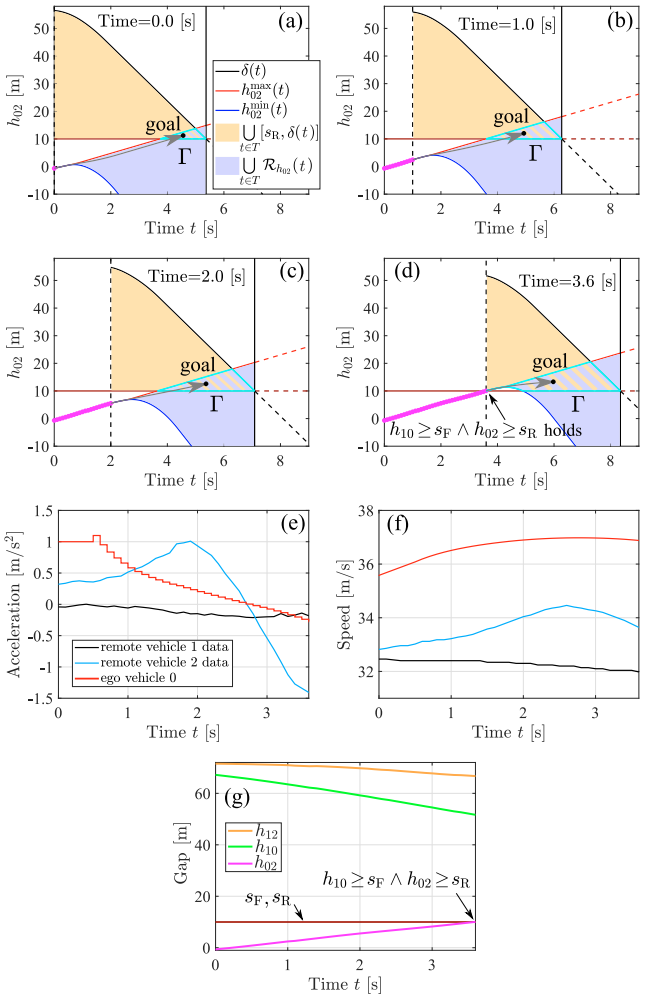

Fig. 5. (a)-(d) Evolution of opportunity set Γ, goal point, and trajectory $h_{02}(t)$ under delays $\sigma = 0.5\,[\mathrm{s}]$ and $\tau = 0.1\,[\mathrm{s}]$ using controller $u_0(t) = u_0^{\mathrm{G}}$ with status updates in every 0.1 [s]. (e)-(g) Simulation results.

REFERENCES

Albaba, B.M. and Yildiz, Y. (2019). Modeling cyber-physical human systems via an interplay between reinforcement learning and game theory. *Annual Reviews in Control*, 48, 1–21.

Bajcsy, A., Herbert, S.L., Fridovich-Keil, D., Fisac, J.F., Deglurkar, S., Dragan, A., and Tomlin, C. (2019). A scalable framework for real-time multi-robot, multi-human collision avoidance. *2019 International Conference on Robotics and Automation (ICRA)*, 936–943.

Haddad, S. and Halder, A. (2020). The convex geometry of integrator reach sets. In *2020 American Control Conference (ACC)*, 4466–4471.

Hafner, M.R., Cunningham, D., Caminiti, L., and Del Vecchio, D. (2013). Cooperative collision avoidance at

intersections: Algorithms and experiments. *IEEE Transactions on Intelligent Transportation Systems*, 14(3), 1162–1175.

Karimi, M., Roncoli, C., Alecsandru, C., and Papageorgiou, M. (2020). Cooperative merging control via trajectory optimization in mixed vehicular traffic. *Transportation Research Part C*, 116, 102663.

Kochdumper, N. and Althoff, M. (2021). Sparse polynomial zonotopes: A novel set representation for reachability analysis. *IEEE Transactions on Automatic Control*, 66(9), 4043–4058.

Liu, C., Lin, C.W., Shiraishi, S., and Tomizuka, M. (2020). Distributed conflict resolution for connected autonomous vehicles. *IEEE Transactions on Intelligent Vehicles*, 3(1), 18–29.

Rios-Torres, J. and Malikopoulos, A.A. (2016). A survey on the coordination of connected and automated vehicles at intersections and merging at highway on-ramps. *IEEE Transactions on Intelligent Transportation Systems*, 18(5), 1066–1077.

SAE J2735 (2016). Dedicated Short Range Communications (DSRC) Message Set Dictionary Set. Technical report, SAE International.

SAE J3016 (2021). Taxonomy and Definitions for Terms Related to Driving Automation Systems for On-Road Motor Vehicles. Technical report, SAE International.

SAE J3216 (2021). Taxonomy and Definitions for Terms Related to Cooperative Driving Automation for On-Road Motor Vehicles. Technical report, SAE International.

Wang, H.M., Avedisov, S.S., Altintas, O., and Orosz, G. (2022a). Multi-vehicle conflict management with status and intent sharing. In *2022 IEEE Intelligent Vehicles Symposium (IV)*, 1321–1326.

Wang, H.M., Avedisov, S.S., Molnár, T.G., Sakr, A.H., Altintas, O., and Orosz, G. (2022b). Conflict analysis for cooperative maneuvering with status and intent sharing via V2X communication. *IEEE Transactions on Intelligent Vehicles*. Published online.

Wang, H.M., Avedisov, S.S., Sakr, A.H., Altintas, O., and Orosz, G. (2021). Opportunistic strategy for cooperative maneuvering using conflict analysis. In *2021 IEEE Intelligent Vehicles Symposium (IV)*, 348–353.

Wang, H.M., Molnár, T.G., Avedisov, S.S., Sakr, A.H., Altintas, O., and Orosz, G. (2020). Conflict analysis for cooperative merging using V2X communication. In *2020 IEEE Intelligent Vehicles Symposium (IV)*, 1538–1543.

Appendix A. ANALYTICAL FORMS OF $\delta(t)$, $h_{02}^{\min}(t)$, AND $h_{02}^{\max}(t)$

$\delta(t) = r_1^*(t) - r_2^*(t) - s_{\mathrm{F}} - 2l$, where

$$r_1^*(t) = g(r_1(0), v_1(0), a_{\min,1}, v_{\min,1}, t), \tag{A.1}$$

$$r_2^*(t) = g(r_2(0), v_2(0), a_{\max,2}, v_{\max,2}, t), \tag{A.2}$$

$$g(r_2(0), v_2(0), a_{\max,2}, v_{\max,2}, t) = \tag{A.3}$$

$$\begin{cases} r_2(0)+v_2(0)t+\dfrac{1}{2}a_{\max,2}t^2 & \text{if } t \le \dfrac{(v_{\max,2}-v_2(0))}{a_{\max,2}}, \\ r_2(0)-\dfrac{(v_{\max,2}-v_2(0))^2}{2a_{\max,2}}+v_{\max,2}t & \text{otherwise,} \end{cases}$$

and $h_{02}^{\min}(t) = r_0^*(t) - \underline{r}_2^*(t) - l$, $h_{02}^{\max}(t) = r_0^*(t) - \bar{r}_2^*(t) - l$, where

$$\underline{r}_0^*(t) = \begin{cases} \tilde{g}(r_0(0), v_0(0), t) & \text{if } t \le \sigma, \\ g(r_0(\sigma), v_0(\sigma), a_{\min,0}, v_{\min,0}, t-\sigma) & \text{otherwise,} \end{cases} \tag{A.4}$$

$$\bar{r}_0^*(t) = \begin{cases} \tilde{g}(r_0(0), v_0(0), t) & \text{if } t \le \sigma, \\ g(r_0(\sigma), v_0(\sigma), a_{\max,0}, v_{\max,0}, t-\sigma) & \text{otherwise,} \end{cases} \tag{A.5}$$

$$\tilde{g}(r_0(0), v_0(0), t) = r_0(0) + v_0(0)\sigma + \int_0^t \int_0^{\bar{t}} \mathrm{sat}(u(\tilde{t}-\sigma))\mathrm{d}\tilde{t}\mathrm{d}\bar{t}, \tag{A.6}$$

$$r_0(\sigma) = \tilde{g}(r_0(0), v_0(0), \sigma), \tag{A.7}$$

$$v_0(\sigma) = v_0(0) + \int_0^{\sigma} \mathrm{sat}(u(\tilde{t}-\sigma))\mathrm{d}\tilde{t}. \tag{A.8}$$

Note that with communication delay, one needs to replace $r_1(0)$, $v_1(0)$, $r_2(0)$, and $v_2(0)$ in (A.1) and (A.2) with their estimated values based on (15) and (16).

Appendix B. PROOF OF THEOREM 1

If $\Gamma \neq \emptyset$, then from the definition of Γ in (11), under $(u_1, u_2) \equiv (a_{\min,1}, a_{\max,2})$, one obtains $\exists u_0, \exists t \in T, s_{\mathrm{R}} \le h_{02}(t) \le \delta(t)$. Substituting $\delta(t) = h_{12}(t) - s_{\mathrm{F}} - l$ yields $h_{02}(t) \le h_{12}(t) - s_{\mathrm{F}} - l$, i.e., $s_{\mathrm{F}} \le h_{10}(t)$. These and Lemma 1 give $\mathbf{x}(0) \in \mathcal{P}_{\mathrm{g}}$.

If $\Gamma = \emptyset$, then under $(u_1, u_2) \equiv (a_{\min,1}, a_{\max,2})$, one obtains $\forall u_0(t), \forall t \in T, \neg\{s_{\mathrm{R}} \le h_{02}(t) \le \delta(t)\}$, i.e., $\neg\{h_{10}(t) \ge s_{\mathrm{F}} \wedge h_{02}(t) \ge s_{\mathrm{R}}\}$. $\forall t \notin T$, one still has $\neg\{h_{10}(t) \ge s_{\mathrm{F}} \wedge h_{02}(t) \ge s_{\mathrm{R}}\}$. Thus, for $(u_1, u_2) \equiv (a_{\min,1}, a_{\max,2})$, $\forall u_0, \neg P$. This leads to $\mathbf{x}(0) \notin \mathcal{P}_{\mathrm{g}}$.

Appendix C. CONTROLLER u_0^{G}

Given a goal point $(t^{\mathrm{G}}, h_{02}^{\mathrm{G}}) \in \Gamma$, we have

$$u_0^{\mathrm{G}} = \begin{cases} \dfrac{2(s^{\mathrm{G}} - (t^{\mathrm{G}}-\sigma)v_0)}{(t^{\mathrm{G}}-\sigma)^2}, \text{ if } s^{\mathrm{G}} \in [\dfrac{(t^{\mathrm{G}}-\sigma)(v_0+v_{\min,0})}{2}, \\ \qquad\qquad \dfrac{(t^{\mathrm{G}}-\sigma)(v_0+v_{\max,0})}{2}], \\ f_1(v_0, t^{\mathrm{G}}, s^{\mathrm{G}}), \quad \text{if } s^{\mathrm{G}} \in [0, \dfrac{(t^{\mathrm{G}}-\sigma)(v_0+v_{\min,0})}{2}], \\ f_2(v_0, t^{\mathrm{G}}, s^{\mathrm{G}}), \qquad \text{otherwise,} \end{cases} \tag{C.1}$$

where s^{G} is the distance that the ego vehicle must travel for $t > \sigma$ to secure rear gap h_{02}^{G} at t^{G} assuming the worst-case behavior of remote vehicle 2. That is, $s^{\mathrm{G}} = r_2^*(t^{\mathrm{G}}) - r_0(\sigma) + h_{02}^{\mathrm{G}} + l$ for the $r_2^*(\cdot)$ in (A.2) and $r_0(\sigma)$ in (A.7). Moreover, we also have

$$f_1(v_0, t^{\mathrm{G}}, s^{\mathrm{G}}) = \begin{cases} \dfrac{2(s^{\mathrm{G}} - (t^{\mathrm{G}}-\sigma)v_0)}{(t^{\mathrm{G}}-\sigma)^2}, \text{ if } a_{\min,0} \ge \dfrac{v_{\min,0}-v_0}{t^{\mathrm{G}}-\sigma}, \\ \dfrac{(v_0 - v_{\min,0})^2}{2((t^{\mathrm{G}}-\sigma)v_{\min,0} - s^{\mathrm{G}})}, \text{ otherwise,} \end{cases} \tag{C.2}$$

$$f_2(v_0, t^{\mathrm{G}}, s^{\mathrm{G}}) = \begin{cases} \dfrac{2(s^{\mathrm{G}} - (t^{\mathrm{G}}-\sigma)v_0)}{(t^{\mathrm{G}}-\sigma)^2}, \text{ if } a_{\max,0} \le \dfrac{v_{\max,0}-v_0}{t^{\mathrm{G}}-\sigma}, \\ \dfrac{(v_0 - v_{\max,0})^2}{2((t^{\mathrm{G}}-\sigma)v_{\max,0} - s^{\mathrm{G}})}, \text{ otherwise.} \end{cases} \tag{C.3}$$